

## Supporting Information for

# Anisotropy of the n-type charge transport and thermal effects in crystals of a fluoro-alkylated naphthalene diimide: a computational investigation.

Sofia Canola, Fabrizia Negri\*

<sup>a</sup>Università di Bologna, Dipartimento di Chimica ‘G. Ciamician’,

Via F. Selmi, 2, 40126 Bologna, Italy and INSTM, UdR Bologna, Italy.

## Details on Computational Methods.

Two parameters govern the hopping process: the charge transfer integral or electronic coupling  $V_{ij}$  between the two molecules i and j forming the dimer and the reorganization energy  $\lambda$ . The electronic couplings  $V'_{ij}$  were computed at B3LYP/6-31G\* level of theory (or B3LYP/3-21G level for the evaluation of fluctuations) in the one-electron approximation, following the direct approach described in previous work.<sup>1-3</sup> The computed  $V'_{ij}$  were transformed in an orthogonalized basis ( $V_{ij}$ ) as described in previous studies.<sup>4</sup> The reorganization energy is composed by an intra-molecular contribution  $\lambda_i$  and an outer contribution  $\lambda_o$  arising from the embedding of the molecular dimer in the crystal.

$$\lambda = \lambda_i + \lambda_o \quad (\text{S1})$$

The intramolecular contribution to the reorganization energy  $\lambda_i$  was computed with the B3LYP functional, either with the adiabatic potential (AP) approach<sup>5-8</sup> (see Figure S1 and Tables S1-S3) or via calculations of Huang-Rhys (HR) parameters  $S_m$ <sup>5,6</sup> (see Tables S4-S5), in turn obtained from the dimensionless displacement parameters  $B$  usually employed in the evaluation of the Franck-Condon (FC) vibronic progressions in electronic spectra.<sup>9,10</sup> The latter, assuming the harmonic approximation and neglecting Duschinski rotation, are defined as

$$B_m = \sqrt{\frac{\omega_m}{\hbar}} \{ \mathbf{X}_K - \mathbf{X}_J \} \mathbf{M}^{1/2} \mathbf{L}_m(K)$$

$$S_m = \frac{1}{2} B_m^2 \quad (\text{S2})$$

where  $\mathbf{X}_{K,J}$  is the  $3N$  dimensional vector of the equilibrium Cartesian coordinates of the  $K,J$ th state (here the neutral and charged molecular states),  $\mathbf{M}$  is the  $3N \times 3N$  diagonal matrix of the atomic masses and  $\mathbf{L}_m(K)$  is the  $3N$  vector describing the normal coordinate  $Q_m$  of the  $K$  state in terms of mass-weighted Cartesian coordinates.

$k_{eT}$  were computed according to Marcus-Levich-Jortner (MLJ) formulation.<sup>11,12</sup> The effective frequency was determined as

$$\omega_{eff} = \sum_m \omega_m \frac{S_m}{\sum_n S_n} \quad (S3)$$

The HR factor  $S_{eff}$  was obtained from the relation  $\lambda_i = \hbar \omega_{eff} S_{eff}$ .

**Table S1** Absolute energies of the neutral and charged species employed to evaluate the intramolecular reorganization energies according to the AP method along with vertical and adiabatic EAs.

B3LYP/6-31+G*	$E_n^{geo-n}$	$E_a^{geo-a}$	$E_n^{geo-a}$	$E_a^{geo-n}$
<b>tFNDI</b>	-2651.544041	-2651.651260	-2651.537066	-2651.644200
<b>cFNDI</b>	-2651.541819	-2651.648976	-2651.534679	-2651.641839
<b>HNDI</b>	-947.639177	-947.735795	-947.633128	-947.729660

**Table S2** VEAs, AEAs and intramolecular reorganization energies  $\lambda_i$  for **tFNDI**, **cFNDI** and **HNDI** computed at the B3LYP/6-31+G\* level of theory.

B3LYP/6-31+G*	$VEAn / eV$	$VEAc / eV$	$AEA / eV$	$\lambda_i = (VEAc - VEAn)$
<b>tFNDI</b>	2.72	3.11	2.92	0.382
<b>cFNDI</b>	2.72	3.11	2.92	0.388
<b>HNDI</b>	2.46	2.79	2.63	0.332

**Table S3** Adiabatic Potential (AP) intramolecular reorganization energies (eV) computed for the systems investigated at B3LYP/6-31+G\*.

B3LYP/6-31+G*	$\lambda_i^{n(AP)} \text{ a}$	$\lambda_i^{a(AP)} \text{ b}$	$\lambda_i^{AP}$
<b>tFNDI</b>	0.192	0.190	0.382
<b>cFNDI</b>	0.194	0.194	0.388
<b>HNDI</b>	0.165	0.167	0.332

<sup>a</sup> contribution from the neutral system, computed according to the AP method. <sup>b</sup> contribution from the charged system, computed according to the AP method. See also Figure S1 for a graphical representation of the reorganization energies.

**Table S4** Computed vibrational contributions to the intra-molecular reorganization energy for **tFNDI**

Neutral state			Anionic state		
v [cm <sup>-1</sup> ]	S	$\lambda_i$ [cm <sup>-1</sup> ]	v [cm <sup>-1</sup> ]	S	$\lambda_i$ [cm <sup>-1</sup> ]
12	0,07179	1	12	0,08815	1
23	0,17104	4	23	0,11648	3
24	1,12274	27	25	1,20962	31
53	0,00011	0	77	0,00015	0
75	0,00038	0	100	0,01061	1
95	0,00167	0	106	0,06667	7
104	0,03042	3	112	0,00112	0
105	0,10137	11	180	0,02483	4

176	0,05258	9		213	0,0001	0
212	0,00072	0		218	0,00527	1
220	0,00315	1		229	0,00018	0
252	0,00046	0		283	0,05689	16
283	0,08719	25		315	0,03301	10
317	0,04914	16		341	0,00346	1
329	0,00057	0		367	0,01924	7
332	0,00069	0		420	0,00035	0
342	0,00077	0		422	0,00203	1
367	0,00315	1		447	0,41806	187
369	0,00087	0		501	0,00081	0
408	0,00011	0		514	0,00869	4
426	0,00096	0		522	0,00025	0
448	0,43491	195		538	0,02918	16
454	0,00012	0		547	0,13091	72
473	0,02174	10		619	0,00021	0
523	0,0002	0		624	0,06299	39
538	0,01252	7		650	0,01543	10
553	0,10679	59		715	0,00259	2
629	0,03762	24		792	0,00547	4
653	0,01372	9		809	0,00012	0
713	0,0033	2		892	0,02438	22
738	0,01024	8		947	0,00037	0
898	0,01351	12		1110	0,00335	4
974	0,00027	0		1112	0,03406	38
1012	0,00032	0		1175	0,00066	1
1100	0,06159	68		1202	0,00513	6
1119	0,00028	0		1273	0,00056	1
1187	0,00221	3		1333	0,01545	21
1220	0,00103	1		1341	0,00621	8
1340	0,01323	18		1383	0,00024	0
1354	0,02406	33		1395	0,20782	290
1405	0,00355	5		1417	0,03887	55
1434	0,00034	0		1448	0,00519	8
1444	0,24355	352		1465	0,00705	10
1474	0,01101	16		1642	0,15843	260
1641	0,21205	348		1713	0,24988	428
1777	0,13862	246				

**Table S5** Vibrational contributions to the intra-molecular reorganization energy for cFNDI

Neutral state			Anionic state		
v [cm <sup>-1</sup> ]	S	λ <sub>i</sub> [cm <sup>-1</sup> ]	v [cm <sup>-1</sup> ]	S	λ <sub>i</sub> [cm <sup>-1</sup> ]
11	2,65326	30	11	2,6937	29
16	0,16684	3	16	0,07965	1

24	0,13895	3		23	0,01606	0
36	0,00384	0		40	0,02117	1
69	0,06899	5		68	0,0182	1
82	0,03278	3		83	0,10836	9
84	0,03939	3		86	0,00583	1
98	0,18156	18		98	0,04534	4
124	0,00029	0		132	0,00119	0
160	0,05989	10		161	0,07976	13
186	0,01366	3		197	0,00784	2
221	0,03516	8		222	0,01602	4
249	0,01901	5		249	0,01693	4
261	0,1765	46		262	0,06839	18
280	0,02349	7		285	0,00094	0
310	0,01086	3		308	0,01861	6
313	0,00082	0		315	0,03422	11
332	0,00091	0		331	0,00739	2
337	0,00214	1		337	0,00564	2
385	0,01403	5		347	0,00038	0
411	0,00029	0		385	0,01427	5
424	0,08336	35		422	0,0639	27
447	0,14509	65		444	0,17775	79
473	0,13766	65		473	0,16252	77
522	0,002	1		521	0,00082	0
545	0,00272	1		544	0,04297	23
552	0,12728	70		547	0,10477	57
583	0,00271	2		580	0,00062	0
596	0,00225	1		594	0,00272	2
631	0,01926	12		627	0,0285	18
657	0,01985	13		654	0,07536	49
731	0,0157	11		729	0,00155	1
757	0,00293	2		748	0,00418	3
797	0,00508	4		793	0,01621	13
828	0,0001	0		846	0,00052	0
900	0,00045	0		934	0,02257	21
938	0,02178	20		946	0,00074	1
952	0,00277	3		974	0,00178	2
975	0,00802	8		1090	0,00186	2
1086	0,01209	13		1115	0,03383	38
1097	0,02101	23		1155	0,00156	2
1108	0,02112	23		1180	0,014	17
1160	0,00138	2		1204	0,00022	0
1183	0,00017	0		1205	0,003	4
1191	0,00239	3		1224	0,00329	4
1233	0,00145	2		1235	0,00704	9
1234	0,00596	7		1262	0,00358	5
1246	0,00013	0		1329	0,01323	18
1333	0,00485	6		1336	0,00073	1
1355	0,02867	39		1390	0,00495	7
1406	0,00399	6		1396	0,20843	291
1436	0,00093	1		1419	0,03453	49
1445	0,24714	357		1449	0,00665	10
1474	0,01226	18		1468	0,00407	6

1642	0,20968	344		1642	0,15997	263
1777	0,14421	256		1665	0,0002	0
				1713	0,24805	425

**Table S6** Eigenvalues and eigenvectors of the mobility tensor of **FNDI** crystals in the absence of applied electric field.

Eigenvalue/ cm <sup>2</sup> /Vs	Eigenvector components		
	x	y	z
<b>0.000</b>	0.98	0.00	0.20
<b>0.631</b>	0.00	-1.00	0.01
<b>1.139</b>	-0.20	-0.01	0.98

**Table S7** Analysis of the electronic coupling fluctuations (computed at B3LYP/3-21G level of theory) in terms of Gaussian distribution parameters

Dimer	$\sigma / \text{cm}^{-1}$	$V_{ij} / \text{cm}^{-1}$
D1	111	548
D2	229	347
D4	28	152
D5	65	206

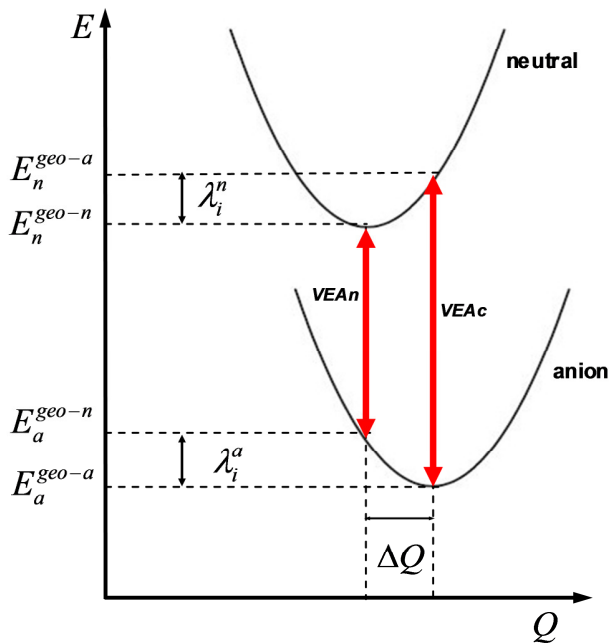


**Figure S1.** Schematic representation of the potential energy curves of neutral and charged species involved in the charge transfer process and indication of the two contributions to the total internal reorganization energy. The scheme, applied to the reduction process suitable for NDI derivatives, also shows the relation between  $VEAn$  and  $VEAc$  and the  $\lambda_i$ .  $E_y^{geo-x}$  represents the energy of the  $y$  state computed at the geometry of the  $x$  state ( $x,y = \text{neutral or charged}$ ).

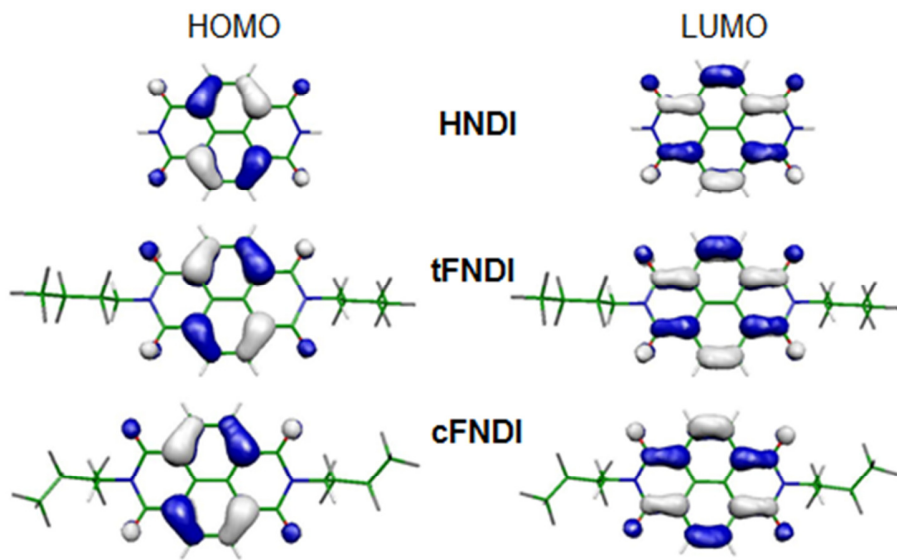


**Figure S2.** The frontier molecular orbitals of **HNDI**, **tFNDI** and **cFNDI** computed at B3LYP/6-31+G\* level of theory. The LUMO orbitals of **tFNDI** and **cFNDI** were involved in the calculations of  $V_{ij}$  charge transfer integrals, computed at B3LYP/6-31G\* level of theory.

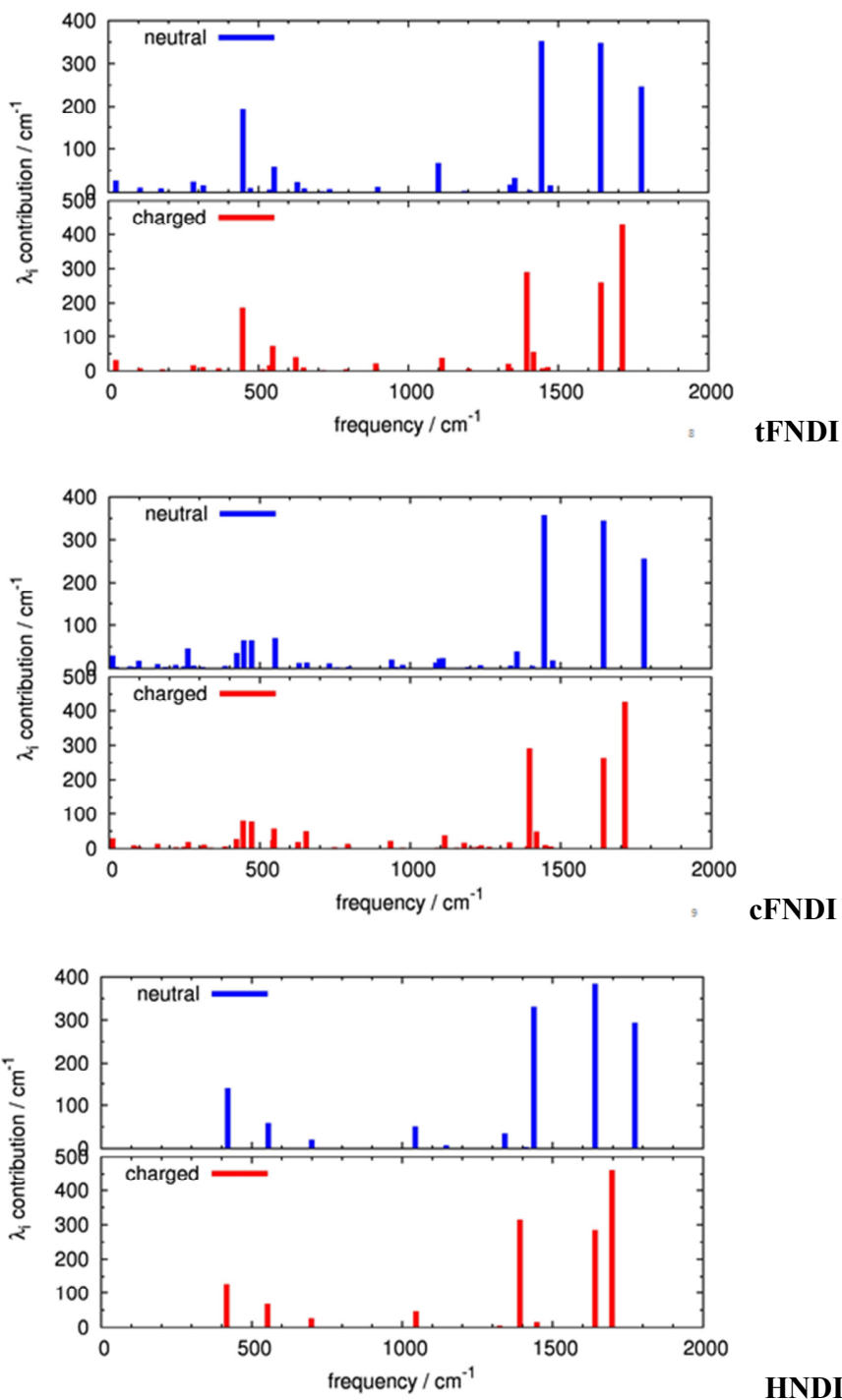


**Figure S3.** The vibrational frequencies contributions to the computed intramolecular reorganization energies of **tFNDI** (top), **cFNDI** (middle) and **HNDI** (bottom). Each graph shows the contribution from neutral species on the top and from the anionic species in the bottom part. From B3LYP/6-31+G\* calculations.

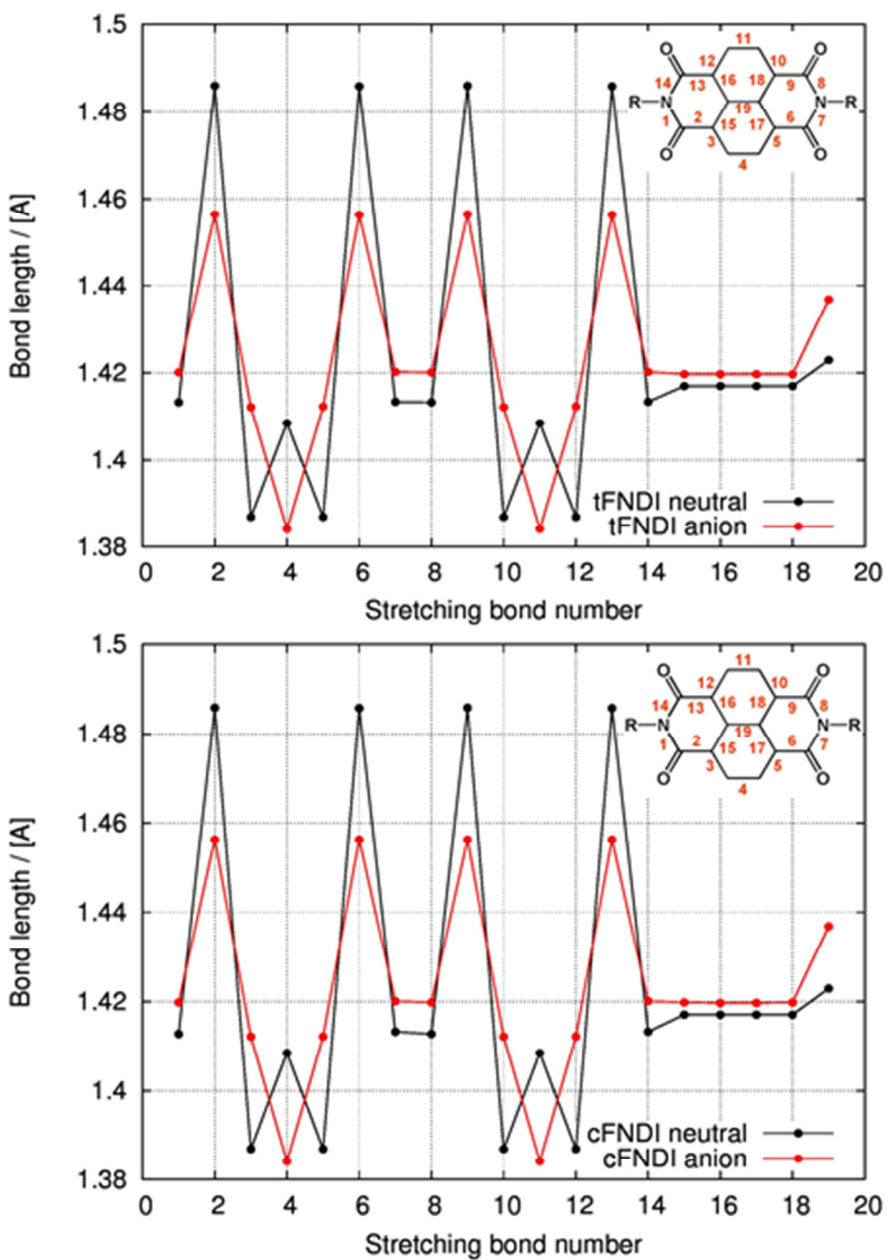


**Figure S4.** Computed bond length (B3LYP/6-31+G\*) for **tFNDI** (top) and **cFNDI** (bottom), neutral structure in black and anionic structure in red. Bond numbering as depicted in the inset.

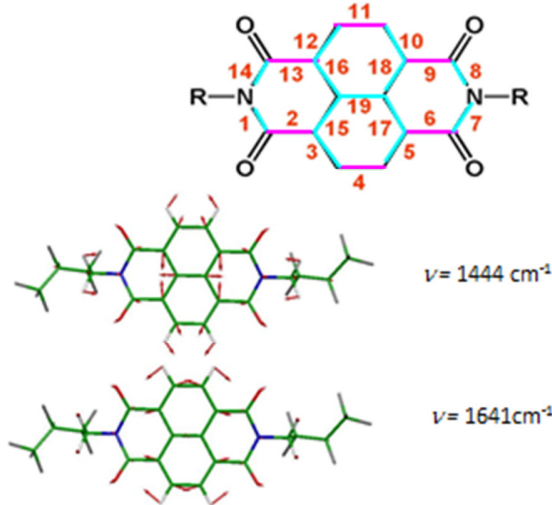


**Figure S5. FNDI:** (top): schematic representation of geometry change upon doping: (magenta) bonds whose length decreases upon doping, (cyan) bonds whose length increases upon doping; (bottom) two of the vibrational modes (neutral species) contributing most to the intramolecular reorganization energy. It can be seen that nuclear motions of the selected vibrations overlap with the computed geometry change.

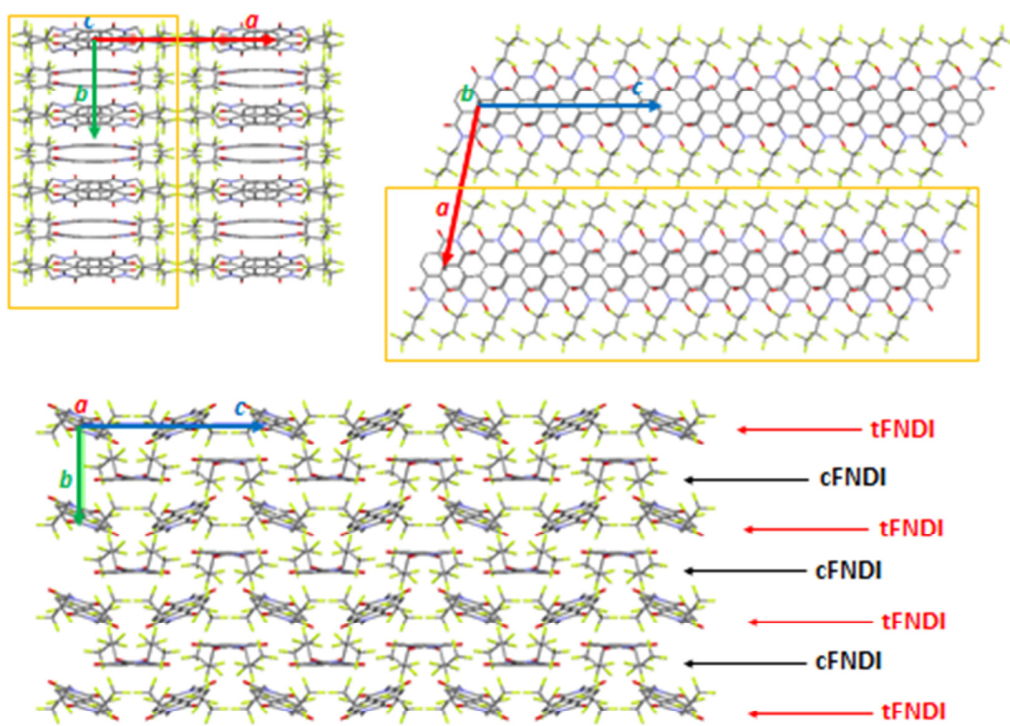


**Figure S6. Molecular crystal of FNDI:** views along crystallographic axes showing the presence of layers (in orange) of  $\pi$ -stacked NDI derivatives and alternating rows of **tFNDI** and **cFNDI** molecules in each layer.

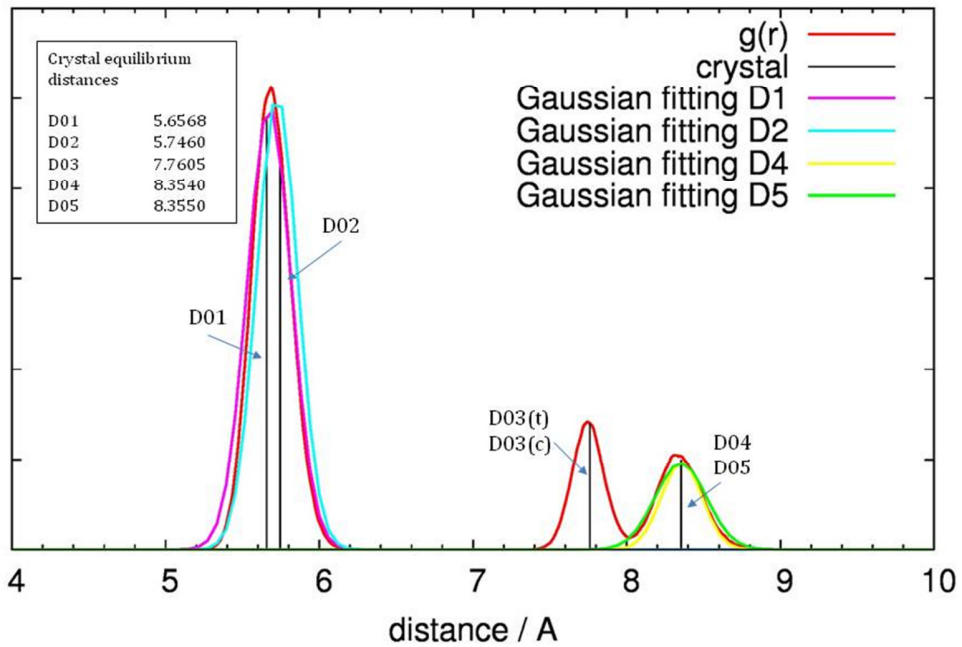


**Figure S7.** FNDI comparison between: (red) Radial distribution function of intermolecular distances between centers of mass, computed from MD simulations at 300 K; (black) center of mass distances computed for the crystal structure. The cyan, magenta, green and yellow curves are Gaussian fittings of the distribution of displacements extracted from MD simulations.

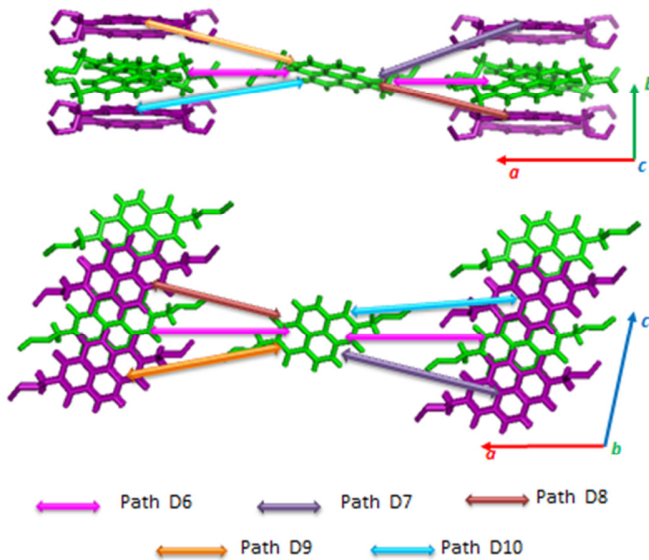


**Figure S8.** Molecular crystal of FNDI: Some possible inter-layer paths taking as reference the green central molecule. These pathways were not included in the KMC simulations since all the couplings were computed to be zero.

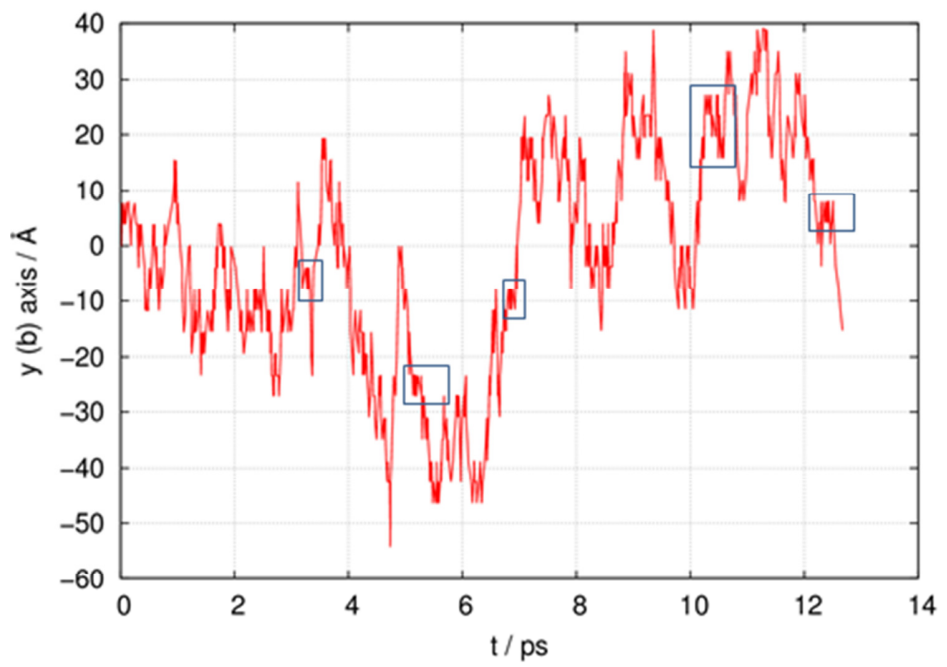


**Figure S9.** A plot of a short trajectory along the *b* crystallographic axis showing (inside rectangular areas) some traces of dimer trapping effects.

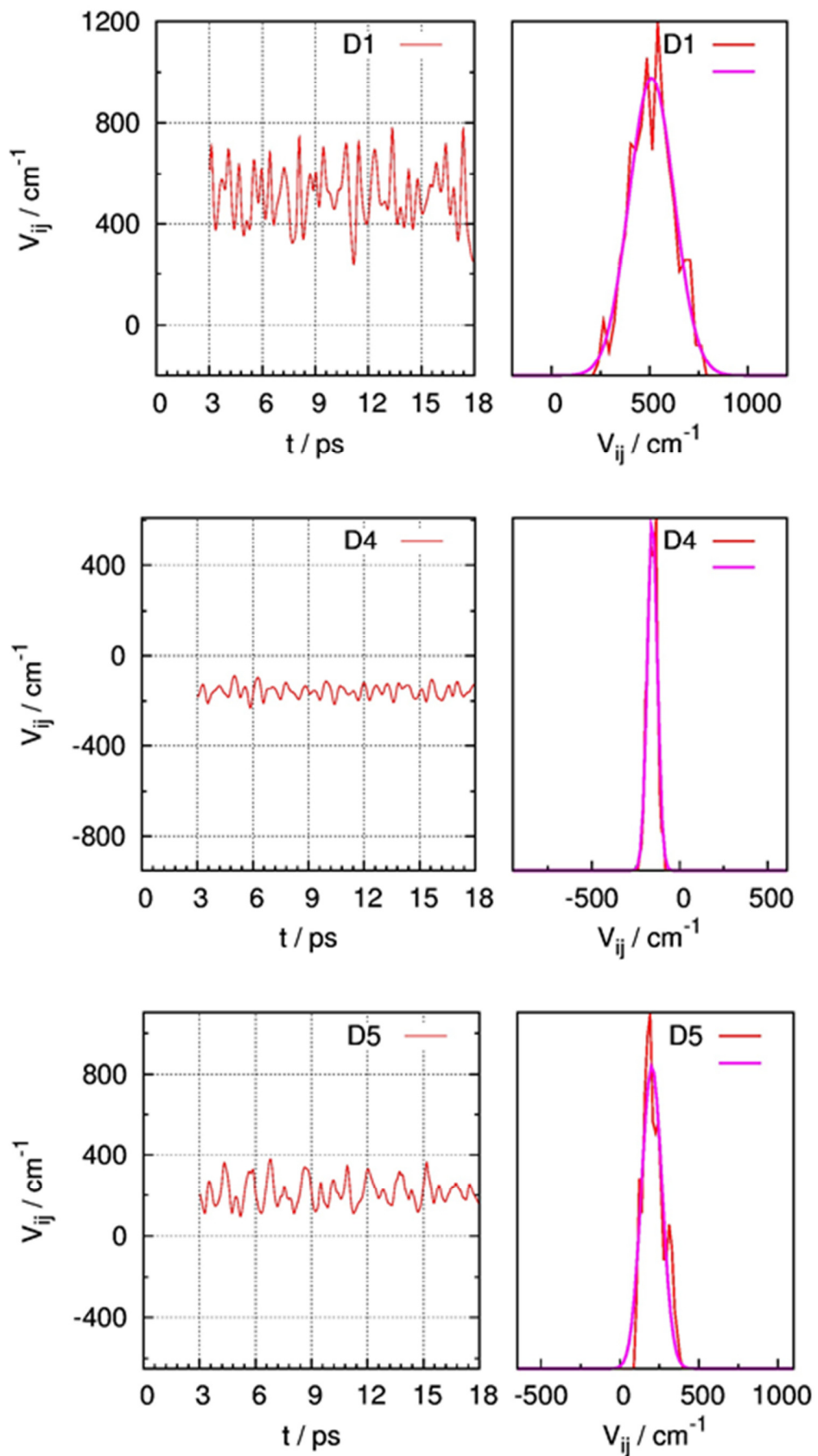


**Figure S10.** Fluctuations and Gaussian distributions for electronic couplings of paths D1, D4 and D5.

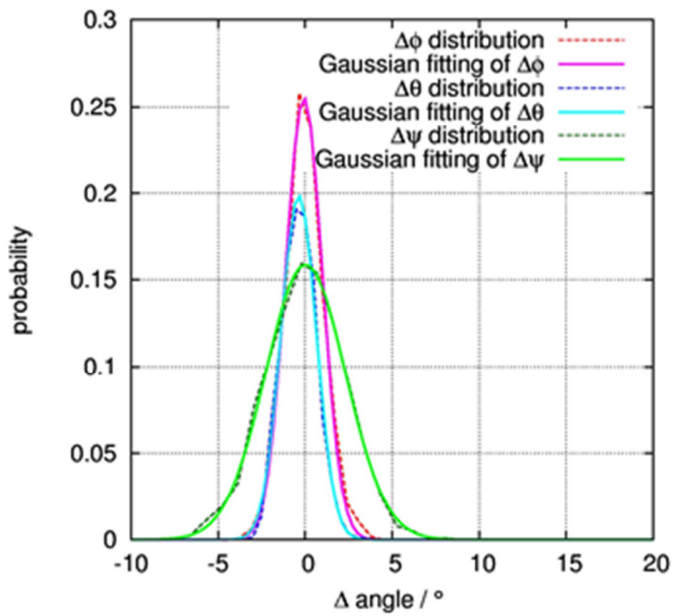


**Figure S11.** Fluctuations and Gaussian fitting of the three Euler angles computed for one of the two molecules forming the D2 dimer. The standard deviation for angle  $\psi$  is larger than for the other two Euler angles. The standard deviations associated with the three angles  $\varphi$ ,  $\theta$  and  $\psi$  are, respectively, 1.05967, 1.01376, 2.30197 degrees.

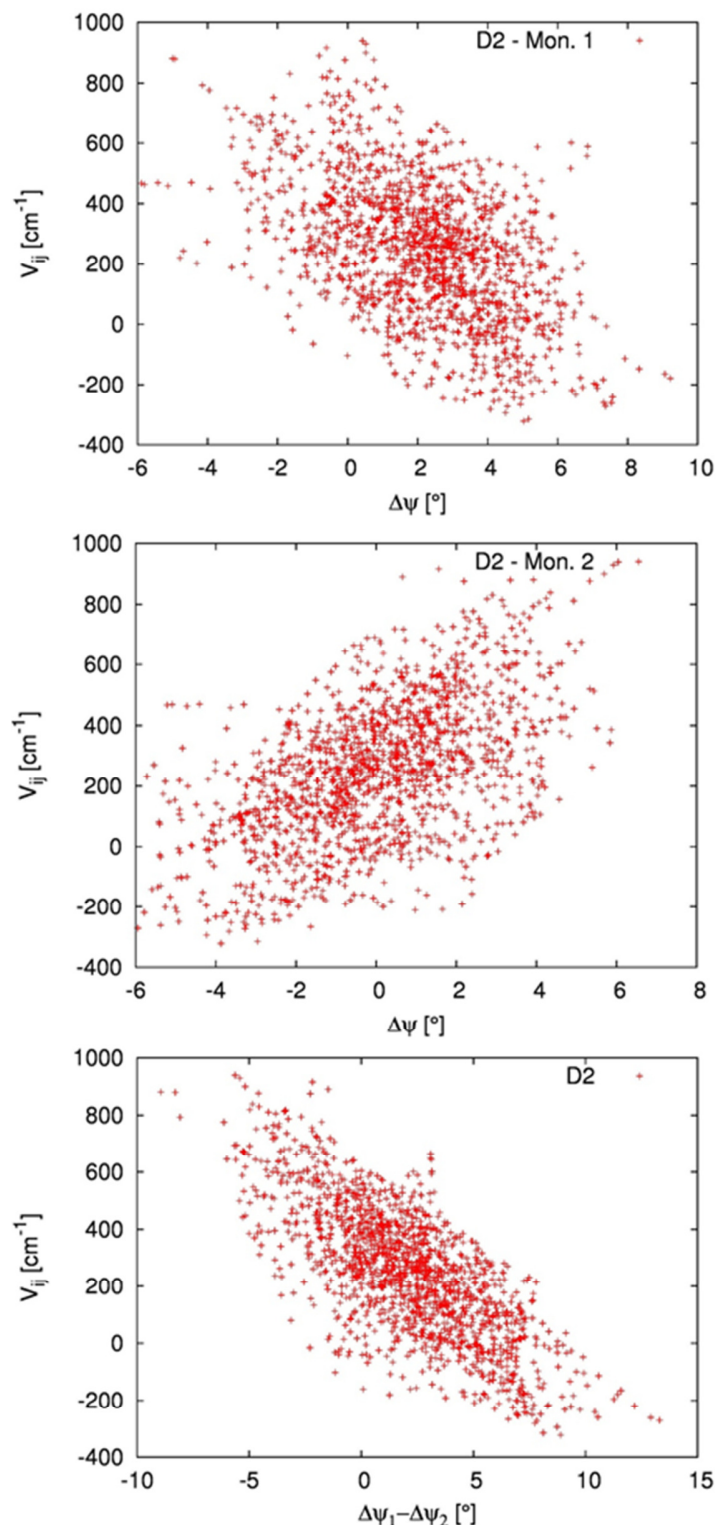


**Figure S12.** Correlation between the fluctuations  $\Delta\psi$  of Euler angle  $\psi$  for (top) monomer 1 (tFNDI) and (middle) monomer 2 (cFNDI) forming the dimer D2, and the electronic coupling  $V_{ij}$  associated with D2. (bottom) Correlation between the out of phase combination ( $\Delta\psi_1 - \Delta\psi_2$ ) of the fluctuations of  $\psi$  for monomer 1 and 2, and the electronic coupling.

## References

- [1]Orlandi, G.; Troisi, A.; Zerbetto, F. *J. Am. Chem. Soc.* **1999**, *121*, 5392-5395.
- [2]Troisi, A.; Orlandi, G. *Chem. Phys. Lett.* **2001**, *344*, 509-518.
- [3]Fujita, T.; Nakai, H.; Nakatsuji, H. *J. Chem. Phys.* **1996**, *104*, 2410-2417.
- [4]Farazdel, A.; Dupuis, M.; Clementi, E.; Aviram, A. *J. Am. Chem. Soc.* **1990**, *112*, 4206-4214.
- [5]Bredas, J. L.; Beljonne, D.; Coropceanu, V.; Cornil, J. *Chem. Rev.* **2004**, *104*, 4971-5003.
- [6]Coropceanu, V.; Andre, J. M.; Malagoli, M.; Bredas, J. L. *Theor. Chem. Acc.* **2003**, *110*, 59-69.
- [7]Fichthorn, K. A.; Weinberg, W. H. *J. Chem. Phys.* **1991**, *95*, 1090-1096.
- [8]Wurthner, F. *Pure Appl. Chem.* **2006**, *78*, 2341-2349.
- [9]Negri, F.; Orlandi, G. *J. Chem. Phys.* **1995**, *103*, 2412-2419.
- [10]Negri, F.; Zgierski, M. Z. *J. Chem. Phys.* **1995**, *102*, 5165-5173.
- [11]Marcus, R. A. *J. Chem. Phys.* **1956**, *24*, 966-978.
- [12]Jortner, J. *J. Chem. Phys.* **1976**, *64*, 4860-4867.